Antibodies formed during primary immune responses suppress germinal center quality upon boosting

Marije F.L. van ‘t Wout

Laboratory of Lymphocyte Dynamics, The Rockefeller University, New York

December 2021 – November 2022

Infection & Immunity Master’s program

Supervisor: Ariën Schiepers
Examiners: Gabriel D. Victora
Balthasar A. Heesters

Table of Contents

Abstract

Upon exposure to foreign antigens, germinal center (GC) responses result in the generation of high-affinity plasma cells and memory B cells, providing long-term protection against infection. Re-exposure to previously encountered antigens typically results in faster and higher affinity antibody responses due to rapid differentiation of memory B cells into antibody-secreting plasma cells. However, to generate antibodies against new epitopes, the generation of high-quality secondary, or 'recall', GCs is desired. Previous studies have shown that antigen-specific antibodies can suppress recall GC quality by blocking antigenic epitopes for naive B cells or promoting Fc-dependent antigen clearance. However, there is still a lot unknown about the effect of prior antigen exposure on recall GC quality and in particular the influence of pre-existing antibodies. By using prime-boost models for the influenza hemagglutinin protein, we show that B cells in recall GCs poorly bind to the immunogen. Recall GC quality could be improved by inhibiting the generation of antibody-producing plasma cells during primary immune responses, supporting the notion that antibody-mediated suppression is an important mechanism by which recall GC quality is reduced. Boosting with variant antigen partially overcomes antibody-mediated suppression, as seen by increased antigen-binding of GC B cells. Interestingly, when mice were immunized with SARS-CoV-2 Spike or hemagglutinin mRNA, recall GC B cells showed similar antigen-binding to primary GC B cells, indicating that mRNA vaccination induces recall GCs of higher quality than protein immunization. Lastly, we studied the contribution of recall GC B cells to serum antibody levels by using a novel 'molecular fate-mapping' approach, in which fate-mapping of immunoglobulin molecules in GC B cells allows us to differentiate between antibodies formed in primary and recall responses. We show that there is little contribution of recall GC B cells to antigen-specific antibody levels, even upon mRNA vaccination, while memory B cells from the primary response are potently engaged. In the future, these insights into the mechanisms governing recall GC quality can be used to improve booster vaccination strategies.

Introduction

An important feature of the adaptive immune system is the generation of long-term protection against infections mediated by B cell-derived antibodies. Naive B cells can bind an almost infinite variety of potential antigens, as each naive B cell encodes a unique immunoglobulin molecule, expressed on the surface as B cell receptors (BCRs). Upon exposure to foreign antigens, naive B cells with the ability to bind these antigens though their BCR can clonally expand and differentiate into memory B cells or plasma cells, which secrete their immunoglobulin molecules as antibodies (1). After binding and internalizing antigen, naive B cells can present antigen-derived peptides to T helper cells that provide T cell help and trigger B cell activation (2,3). Activated B cells either rapidly differentiate into short-lived plasma cells at extrafollicular sites or participate in germinal center (GC) responses, during which the specificity of their BCRs can be fine-tuned. Extrafollicular responses are generally of short duration and result in a short wave of plasma cells, mainly producing IgM antibodies of relatively low affinity. However, the pentameric structure of IgM promotes binding through avidity, as these antibodies can bind antigen with ten instead of two binding sites.

GC responses take longer to develop than extrafollicular responses, but they generate plasma cells of higher affinity through affinity maturation (4). This process is caused by somatic hypermutation, which leads to the diversification of BCRs, followed by positive selection of B cells with the highest affinity (1). Somatic hypermutation is driven by the expression of activation-induced cytidine deaminase (AID), which is also responsible for class-switch recombination from an IgM to an IgG, IgE or IgA isotype (5–7). Positive selection of high-affinity B cells occurs by competition for binding and uptake of antigen, which is held by follicular dendritic cells (FDCs) in the form of immune complexes bound to Fc and complement receptors. Only B cells with the relatively highest affinity will be able to bind and internalize antigen, outcompeting lower affinity B cells. While low-affinity B cells die by neglect, high-affinity cells can present antigenic peptides to follicular T helper cells and receive survival signals. Eventually, B cells with the highest affinity differentiate into plasma cells, which is driven by the expression of the transcription factor Blimp-1 (8). B cells can also differentiate into memory B cells, which are on average of lower affinity but more clonally diverse than plasma cells (9–13).

Re-exposure to a previously encountered antigen typically results in faster and higher affinity antibody responses than the first exposure. Upon secondary, also called ‘recall’, antigen exposure, MBCs quickly proliferate and differentiate into antibody-secreting plasma cells, resulting in a rapid increase in antibody titers (11,12). MBCs could also further optimize their BCR in secondary GCs, but this process was shown to be relatively rare, with recall GCs being primarily formed by naive B cells (14). While secondary exposure to the same antigen efficiently triggers MBC differentiation and amplification of antigen-specific antibody levels, exposure to different antigenic variants often desires the induction of new GCs, activating naive B cells specific for the variant. However, exposure to variant antigens is sometimes associated with reduced antibody responses by preferentially eliciting antibodies against the first encountered antigen (15–18). The term antigenic imprinting, originally described as original antigenic sin (19), refers to the phenomenon that exposure to a new viral strain generates higher antibody titers against antigenic variants encountered earlier in life than to new exposure strains (15). This observation has primarily been described for influenza (20–22), but has also been observed for other viruses such as SARS-CoV-2 (23–26). A skewed immune response toward the first encountered antigen can partly be explained by preferential boosting of cross-reactive MBCs over the induction of new antibodies, resulting in relatively lower immune responses

against the new variant (15–18). Favored activation of MBCs compared to naive B cells could be caused by higher numbers of antigen-specific MBCs than naive B cells and possibly lower activation thresholds (27,28). However, although MBC activation can initially explain the presence of higher titers against the first encountered antigen, it is still unclear whether and to what extent *de novo* immune responses against new antigens are suppressed (15–18).

Many studies have shown that antigen-specific antibodies affect recall immune responses. Pre-existing antibodies can both suppress and enhance antibody responses, depending on antibody characteristics such as isotype and affinity (29,30). On one hand, the formation of antigen-antibody complexes enhances GC responses by increasing antigen loading on FDCs and by promoting antigen uptake by dendritic cells, which can activate T helper cells (30–32). However, antibodies derived from previous exposures can also inhibit the formation of new antibodies. Antibody-mediated suppression of antibody responses was first shown when passive administration of diphtheria toxin-specific antibodies inhibited the generation of antibodies in guinea pigs (33). Now, many studies have shown evidence that antigen-specific antibodies can suppress immune responses (29). There are two hypotheses that could explain these observations. First, pre-existing antibodies can bind antigenic epitopes and thereby prevent recognition by B cells, which is known as 'epitope masking' (34,35). Secondly, antigen-antibody complexes are removed through Fc-dependent clearance, reducing the amount of available antigen (35). Although epitope masking and antigenic clearance are not mutually exclusive (36), epitope masking is thought to be the most important mechanism for antibody-mediated suppression. For instance, passive administration of NP- or SRBC-specific antibodies before immunization with 4-hydroxy-3-nitrophenyl acetyl (NP) coupled to sheep red blood cells (SRBC) suppressed antibody responses in an epitope-specific manner, as NP-specific antibodies only suppressed NP-specific responses, while SRBC-specific antibodies only suppressed SRBC-specific responses (35). Although administration of SRBC-specific IgG did decrease antigen concentrations in the spleen, Fc-dependent clearance seemed to be less important than epitope masking, as suppression was also seen in mice lacking Fc receptors (35).

Observations of suboptimal antibody responses upon variant boosting or administration of antigen-specific antibodies suggest that the quality of GCs is reduced in these settings. Recently, it was shown that prior antigen exposure can have contrasting effects on GC quality. When naive monoclonal B cells were adoptively transferred into previously immunized mice, recruitment of these B cells into secondary GCs was either enhanced or inhibited (37). B cell recruitment was enhanced when primary responses generated low titers of low-affinity, broad-binding antibodies, while recruitment was inhibited when high-affinity, epitope-focused antibodies were formed (37). In the latter case, transfer of immune serum IgG or antigen-specific monoclonal antibodies also inhibited B cell recruitment (37), indicating that antibodies derived from previous responses were responsible impaired B cell recruitment. A similar observation was made when serum from PE-immunized mice was transferred into naive mice, as this reduced the number of PE-binding B cells in GCs upon boosting (38). However, much is still unknown about the effect of prior antigen exposure on recall GC quality and how this is shaped by pre-existing antibodies, especially in non-transfer experiments and in response to complex antigen. Here, we aim to provide additional insights into the role of previous antigen exposure, and pre-existing antibodies in particular, in the quality of recall GCs and serum antibody responses (**Figure 1**). Understanding these principles is important for the design of booster vaccines, as these are often desired to generate new antibodies against novel epitopes.

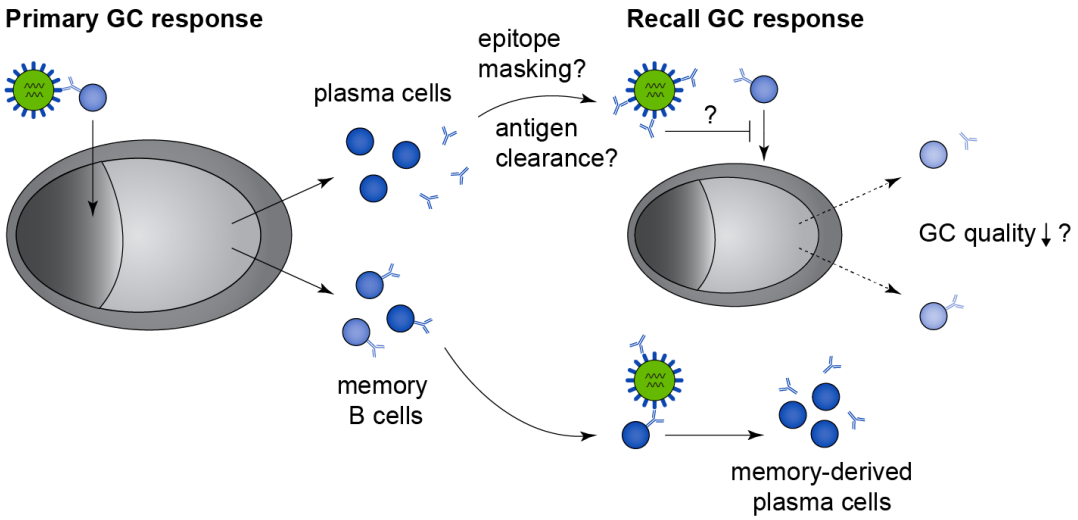

Figure 1: Recall germinal center responses. *Upon primary antigen exposure, naive B cells with the ability to bind this antigen can participate in germinal center (GC) responses, resulting in the generation of antibody-producing plasma cells and memory B cells. Upon secondary exposure to the same antigen, serum antibody levels increase, mainly by the activation of memory B cells. New naive B cells can also be recruited to recall GCs, allowing the generation of antibodies with different specificities. However, primary antibodies potentially reduce recall GC quality by blocking antigenic epitopes and/or promoting antigen clearance, which would prevent activation of naive B cells.*

Results

Prior antigen exposure reduces the quality of recall GCs

First, we compared the quality of primary and recall GCs by using a prime-boost model with the hemagglutinin (HA) protein from H1N1 influenza strain A/Puerto Rico/8/1934 (PR8). Mice were primed by footpad immunization with HA_{PR8} or irrelevant antigen, followed by immunization with HA_{PR8} in the contralateral footpad thirty days later to generate recall or primary GCs, respectively (**Figure 2a**). Popliteal lymph nodes were collected 9 days after secondary immunization and analyzed by flow cytometry (**Supplementary Figure 1**). Primary and recall GCs were similar in size as seen by the number of $Fas^{+}CD38^{low}$ B cells (39,40) (**Figure 2b**), indicating that prior exposure to the same antigen did not affect the number of naive B cells participating in GC responses. However, B cells in recall GCs seemed to be less specific for the immunogen, as they showed less binding to HA_{PR8} tetramers than primary GC B cells (2% vs 10% binding) (**Figure 2c**). The fraction of antigen-binding B cells in recall GCs was still reduced when lymph nodes were collected 14 days after secondary immunization (**Figure 2d**), indicating that antigen-binding GC B cells did not have an obvious competitive advantage over cells that did not show detectable antigen-binding.

To investigate the mechanisms controlling recall GC quality, we first wanted to dissect the role of B and T cell memory on the quality of secondary GCs by immunizing mice with 4-Hydroxy-3-nitrophenylacetyl (NP) hapten-carriers. Since haptens are small molecules, they need to be coupled to a carrier protein to allow B cells to present antigenic peptides on the surface and receive T cell help. As B cell responses to hapten-carriers are focused on the hapten, changing the carrier protein allowed us to dissect the role of B and T cells. GC responses to NP-CGG were analyzed in mice that had been primed with ovalbumin (OVA), NP-CGG or NP-OVA (**Figure 2e**). In absence of T cell memory, when a different carrier protein was used for priming and boosting, the formation of recall GCs was greatly impaired, which was also reflected by less generation of plasma cells compared to primary GCs (**Figure 2f**). When mice were primed and boosted with the same hapten-carriers, GC formation was not affected. These results indicate that previous antigen exposure can inhibit B cell activation and GC formation, but this is overcome by the presence of T cell memory. Similar to our results for HA_{PR8} immunization, NP tetramer binding by GC B cells was reduced compared to primary GCs when boosting with the same hapten-carriers (**Figure 2g**). Unlike B cell responses against most antigens in mice, primary NP responses are characterized by a large proportion of antibodies expressing the Igλ light chain. In our assay, of the B cells that showed detectable binding to NP, a smaller fraction expressed Igλ in recall GCs compared to primary GCs (**Figure 2g)**, suggesting that there is a shift in B cell clones engaged in secondary GC responses. Taken together, these results show that previous antigen exposure reduces the quality of recall GCs, as seen by poor antigen binding capacity and, in absence of T cell memory, smaller GC sizes.

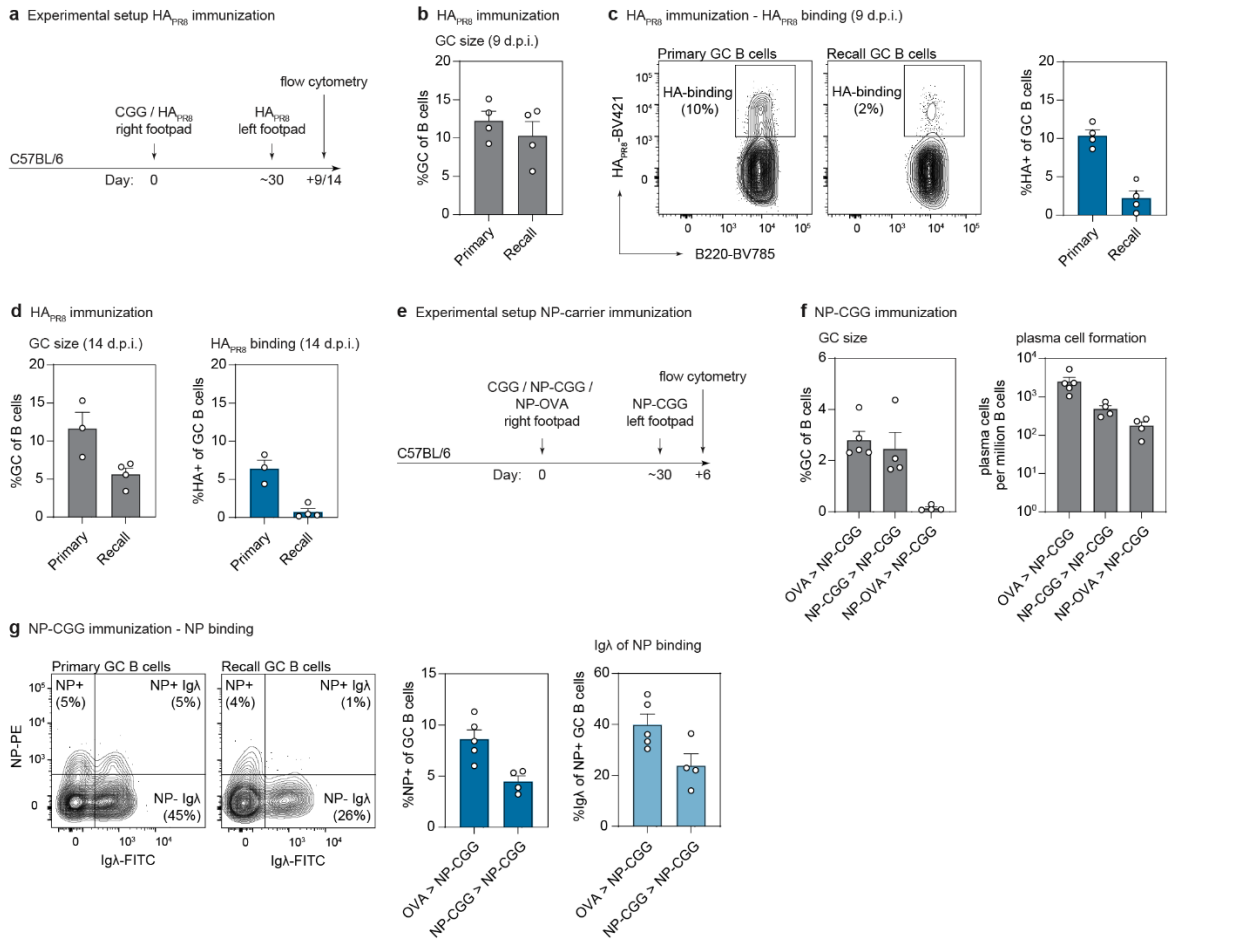

Figure 2: Prior antigen exposure reduces the quality of recall GCs. *(a) Schematic representation of the HA$_{PR8}$ prime-boost model used to generate primary and recall GCs. Mice were primed with chicken gamma globulin (CGG) or HA$_{PR8}$ protein in the right footpad and boosted with HA$_{PR8}$ in the left footpad 1 month later. Left popliteal lymph nodes were collected and analyzed 9 or 14 days post-secondary immunization (d.p.i). (b) Percentage of GC B cells (Fas^{+}CD38^{low}) among total B cells in primary and recall lymph nodes as measured by flow cytometry (Figure S1a). (c) HA$_{PR8}$ tetramer binding by GC B cells as measured by flow cytometry. (d) GC size and HA$_{PR8}$ tetramer binding by primary and recall GCs analyzed 14 days after secondary immunization. (e) Schematic representation of the NP-carrier prime-boost model used to generate primary and recall GCs in presence or absence of T cell memory. (f) GC size and plasma cell formation as measured in Figure S1a 6 days after NP-CGG primary or recall immunization. (g) NP tetramer binding and Igλ fraction of NP-binding GC B cells as measured by flow cytometry. All bar graphs show mean values and error bars represent SEMs.*

Inhibition of primary antibody formation increases recall GC quality

Multiple studies have shown evidence that antigen-specific antibodies can inhibit GC reactions and antibody formation (35,37,38). To test if previously generated antibodies reduced GC quality in our models, we used *AID*^{CreErt2}.*Prdm1*$^{flox/flox}$ (Blimp-flox) mice in which the gene encoding Blimp-1, which drives B cell differentation into plasma cells, is flanked by LoxP sites. By administering tamoxifen during the primary GC response, Blimp-1 will be removed from AID-expressing cells (**Figure 3Figure 2a**). This prevents the generation of plasma cells and primary-derived antibodies without affecting antibodies that are not related to the primary response and that may be important to maintain a steady state. To confirm that antibody formation was successfully inhibited during the primary response, antigen-specific IgG titers were measured at the time of secondary immunization and one week after the boost. After recall NP-CGG immunization, NP titers were about 6-fold lower in Blimp-flox mice compared to littermates without this allele (Blimp-WT) (**Figure 3b**), indicating successful inhibition of plasma cell generation. Removal of Blimp-1 did not affect GC formation, since primary GCs were similar in both size and plasma cell generation between Blimp-WT and Blimp-flox mice (**Figure 3c**). In mice that were primed with NP-OVA and boosted with NP-CGG, recall GCs were bigger and showed increased plasma cell formation in Blimp-flox mice compared to Blimp-WT mice (**Figure 3c**), indicating that antibodies derived from the primary immune response inhibit GC formation. To see if antibodies also affect the antigen-specificity of GC B cells in the more relevant setting of complex protein immunization, we used the same approach for our HA_{PR8} prime-boost model. Again, HA_{PR8} titers were about 5-fold lower in Blimp-flox mice than Blimp-WT mice both before and after the boost (**Figure 3d**). As lymph nodes were collected 2 days earlier than in **Figure 2**, primary GCs were still small, showing that recall GCs are generated faster than primary GCs. Recall GCs were similar in size in Blimp-flox and Blimp-WT mice (**Figure 3e**), but more HA_{PR8} binding was observed in Blimp-flox mice (**Figure 3f**). It was shown before that recall GCs are primarily formed by naive B cells, with only a small fraction being memory-derived (14). To see if pre-existing antibodies also suppress MBC recruitment to GCs, we looked at the re-engagement of MBCs in recall GCs of both Blimp-flox and Blimp-WT mice. As mice possessed the *Rosa26*$^{confetti/confetti}$ allele, tamoxifen administration resulted in fate-mapping of GC B cells and their progenitors as described before (14). Fate-mapping of primary GC B cells showed little memory re-entry in recall GCs of Blimp-WT mice (1% of total GC B cells) (**Supplementary Figure 2**), verifying previous observations (14). More fate-mapped cells were detected in recall GCs of Blimp-flox mice, but was still only 10% of total GC B cells (**Supplementary Figure 2**). Importantly, inhibition of plasma cell formation in the primary response has likely skewed the fate of B cells toward MBC differentiation, which would have resulted in higher numbers of total MBCs. Together, these data show that pre-existing antibodies negatively affect recall GC quality.

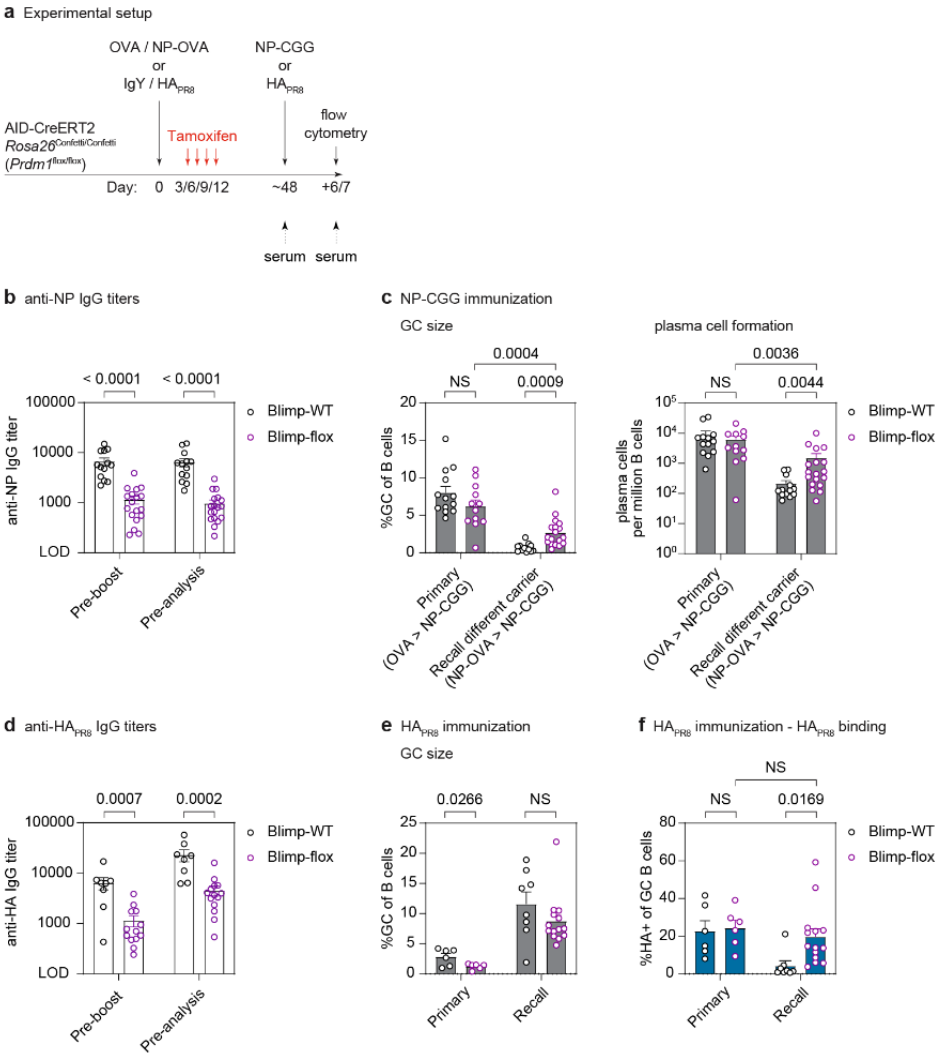

Figure 3: Inhibition of primary antibody formation increases recall GC quality. *(a) Schematic representation of the model to prevent the generation of plasma cells in primary GCs. AID-Confetti mice with or without Blimp-flox allele were primed in the right footpad and boosted in the left footpad on the days indicated by black arrows. Tamoxifen was administered on days 3, 6, 9, and 12 post primary immunization as indicated by red arrows. Serum was collected at the time of secondary immunization and sacrifice. (b) anti-NP IgG titers in serum samples from Blimp-WT and Blimp-flox mice that were primed with NP-OVA and boosted with NP-CGG as measured by ELISA. (c) GC size and plasma cell formation as measured by flow cytometry on day 6 after NP-CGG immunization. (d) anti-HA_{PR8} IgG titers in serum samples from Blimp-WT and Blimp-flox mice that were primed and boosted with HA_{PR8} protein as measured by ELISA. (e) GC size as measured by flow cytometry on day 7 after the last immunization with HA_{PR8} protein. (f) HA_{PR8} tetramer binding by GC B cells as measured by flow cytometry. All bars graphs show mean values and error bars represent SEMs. P-values are shown for unpaired T-tests.*

Boosting with variant antigen partially overcomes suppression of recall GCs

We next wondered to what degree the quality of recall GC responses is affected when boosting with variant antigens. Therefore, we used the HA_{PR8} immunization model of **Figure 2a** and included a heterologously boosted group in which mice were first primed with HA protein from influenza strain A/Fort Monmouth/1/1947 (FM1) (**Figure 4a**), which shares 90% identity with HA_{PR8} at the amino acid level. 9 days after the last immunization, GCs were similar in size (**Figure 4b**). HA_{PR8} binding by GC B cells in heterologously boosted mice was considerably lower compared to primary GC B cells (7% vs 44%), but higher than in homologously boosted mice, in which almost no binding was observed (**Figure 4c**). To confirm the results measured by flow cytometry, we sorted single GC B cells and cultured them in single-cell Nojima cultures (41) to look at antigen-binding of secreted antibodies. Since we did not want to engage the FAS death receptor, GC B cells were sorted based on upregulation of the GL-7 epitope (42) and downregulation of IgD (43) and CD38 (**Supplementary Figure 3**). After culturing for one week, Ig-positive cultures were selected and HA_{PR8} binding of the supernatant was measured by ELISA (**Figure 4d**). To correct for the amount of antibody present in each culture, OD450 nm values for HA_{PR8} binding were divided by the OD450 nm values for total Ig (**Figure 4d**). We then defined high-affinity antibodies as having a ratio above 0.3 and low-affinity antibodies as having a ratio between 0.075 and 0.3. 25% of antibodies secreted by primary GC B cells showed detectable binding to HA_{PR8} after single-cell Nojima culture (**Figure 4d**), which was lower than by flow cytometry, in which 44% binding was observed. For homologously boosted GCs, only 3% of the cultures bound to HA_{PR8} (**Figure 4d**), showing a similar pattern as by flow cytometry. However, although flow cytometry only showed 7% HA_{PR8} binding in heterologously boosted GCs, 16% binding was observed after single-cell Nojima culture, with a large fraction being classified as high-affinity (**Figure 4d**). These results show that boosting with variant antigen partially overcomes suppression of recall GC quality.

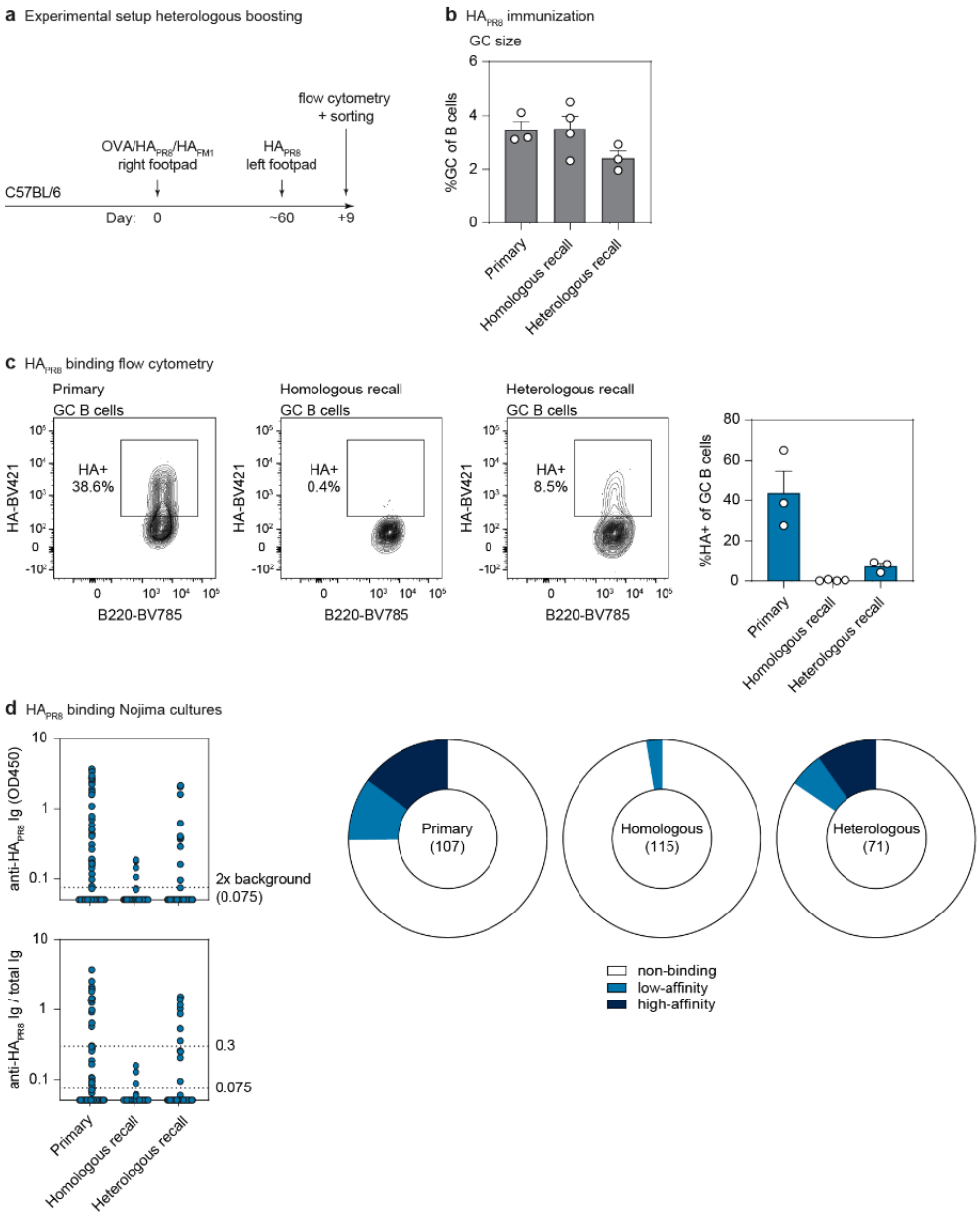

Figure 4: Boosting with variant antigen partially overcomes suppression of recall GCs. *(a) Schematic representation of the HA prime-boost model to generate primary, homologous and heterologous recall GCs. Mice were primed with ovalbumin (OVA), HA_{PR8} or HA_{FM1} protein in the right footpad and boosted with HA_{PR8} in the left footpad 1 month later. Left popliteal lymph nodes were collected and analyzed 9 days after the last immunization. (b) HA_{PR8} tetramer binding by GC B cells as measured by flow cytometry. Bars show mean values and error bars represent SEMs. (c) GC B cells were sorted as shown in Supplementary Figure 3 and cultured in single-cell Nojima cultures. After one week, anti-HA_{PR8} immunoglobulin (Ig) OD450 nm values were measured in the supernatant of Ig-positive cultures by ELISA and divided by total Ig OD450 nm values to correct for the amount of antibody present in each culture. Low- and high-affinity B cells were defined using 0.075 and 0.3 as cutoffs. Fractions of non-binding, low- and high-affinity B cells are shown in pie charts.*

mRNA vaccination induces high-quality recall GCs

To extend these results to another setting, we induced primary and recall GCs by immunization with SARS-CoV-2 Wuhan-Hu-1 Spike mRNA encapsulated in lipid nanoparticles (LNPs), similar to the original SARS-CoV-2 mRNA vaccines (44) (**Figure 5a**). One week after the last immunization, recall GCs were slightly bigger than primary GCs (**Figure 5b**). Surprisingly, similar Spike binding was observed by primary and recall GC B cells (**Figure 5b**), in contrast to our previous findings. To see if this might be a general principle for mRNA immunization, we used the same experimental setup with HA_{PR8} mRNA-LNPs. 9-10 days after the last immunization, recall GCs were only slightly smaller than primary GCs (**Figure 5c**). Again, primary and recall GC B cells showed similar binding to HA_{PR8} (**Figure 5d**). These data show that, in contrast to protein immunization, mRNA vaccination produces high-quality secondary GCs.

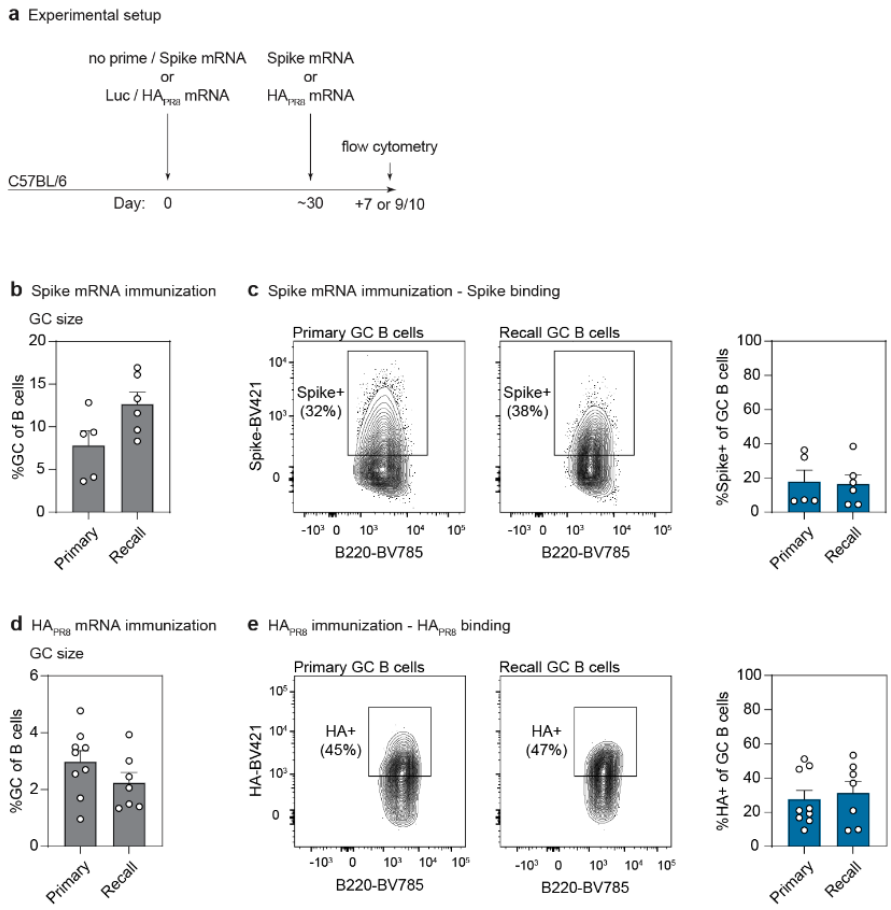

Figure 5: mRNA vaccination induces high-quality recall GCs. *(a) Schematic representation of the mRNA-LNP prime-boost model to generate primary and recall GCs. GCs were analyzed 7 or 9/10 days after the last immunization for Spike and HA_{PR8} mRNA, respectively (b) GC size of primary and recall GCs induced by WH1 Spike mRNA-LNP immunization as measured by flow cytometry. (c) Spike tetramer binding by GC B cells as measured by flow cytometry. (d) GC size of primary and recall GCs induced by HA_{PR8} mRNA-LNP immunization as measured by flow cytometry. (e) HA_{PR8} tetramer binding by GC B cells as measured by flow cytometry. Bar graphs show mean values and error bars represent SEMs.*

GC-derived antibodies are efficiently fate-mapped in Igκ-tag mice

To study the contribution of B cells derived from recall GCs to serum antibody levels, we used the S1pr2-Igκ$^{Tag/Tag}$ (Igκ-tag) mouse model, which was recently developed by the lab (45). In these mice, antibodies derived from GC B cells can be tracked by molecular fate-mapping of the immunoglobulin kappa (Igκ) light chain, which is expressed by >90% of the B cells in mice (45). The C-terminus of the Igκ gene is followed by a LoxP-flanked FLAG-tag, followed by a downstream Strep-tag (**Figure 6a**). Therefore, B cells of Igκ-tag mice express FLAG-tagged antibodies until S1pr2-induced Cre recombinase is activated by tamoxifen, switching the FLAG-tag to a Strep-tag. Since S1pr2 is selectively expressed in GC B cells (46), this method enables fate-mapping of BCRs and antibodies of GC B cells and their progenitors during primary immune responses (**Figure 6b**). To compare titers of FLAG- and Strep-tagged antibodies in serum, IgY-specific monoclonal antibody standards were designed bearing one of both tags. Addition of the FLAG- or Strep-tag did not affect antigen-binding capacity, as they bound IgY equally well as the unmodified monoclonal antibody (**Figure 6c**). In ELISAs, serum titers were defined as the dilution at which each sample reached the OD450 nm value of the FLAG- or Strep-tagged monoclonal antibody at a fixed concentration (**Figure 6d**).

To validate the working of the model, we immunized mice with TNP-KLH in alhydrogel and administered tamoxifen on day 4, 8 and 12 after immunization (**Figure 6b**). TNP was used instead of NP, as our tag is coupled to the Igκ light chain and NP responses are characterized by the engagement of Igλ-expressing B cells. TNP-specific serum IgG titers quickly rose within the first week after immunization, after which they remained relatively stable (**Figure 6e**). When we looked at tag-specific TNP titers, we observed an initial wave of FLAG-tagged antibodies that peaked one week after immunization until they slowly disappeared at 9 weeks post-immunization (**Figure 6e**). While these titers were likely generated by extrafollicular responses, GC-derived Strep-tagged antibodies started to appear one week after immunization and kept increasing (**Figure 6e**). To show that Strep-tagged antibodies were indeed GC-derived, we set up an assay to detect affinity maturation. We produced low and high ratio TNP-BSA conjugates with ~1 or ~13 TNP molecules per BSA protein. In this assay, low-affinity antibodies will only be able to bind to TNP(13)-BSA through avidity, in which antigen is bound by multiple binding sites, while high-affinity antibodies can also bind to TNP(1)-BSA. By calculating the ratio between TNP(1)BSA and TNP(13)BSA binding titers of FLAG- and Strep-tagged antibodies, we show that the average affinity of Strep-tagged antibodies increases over time, which is not the case for FLAG-tagged antibodies (**Figure 6f**). These data demonstrate that the Igκ-tag mouse can be used to efficiently track GC-derived antibodies over time.

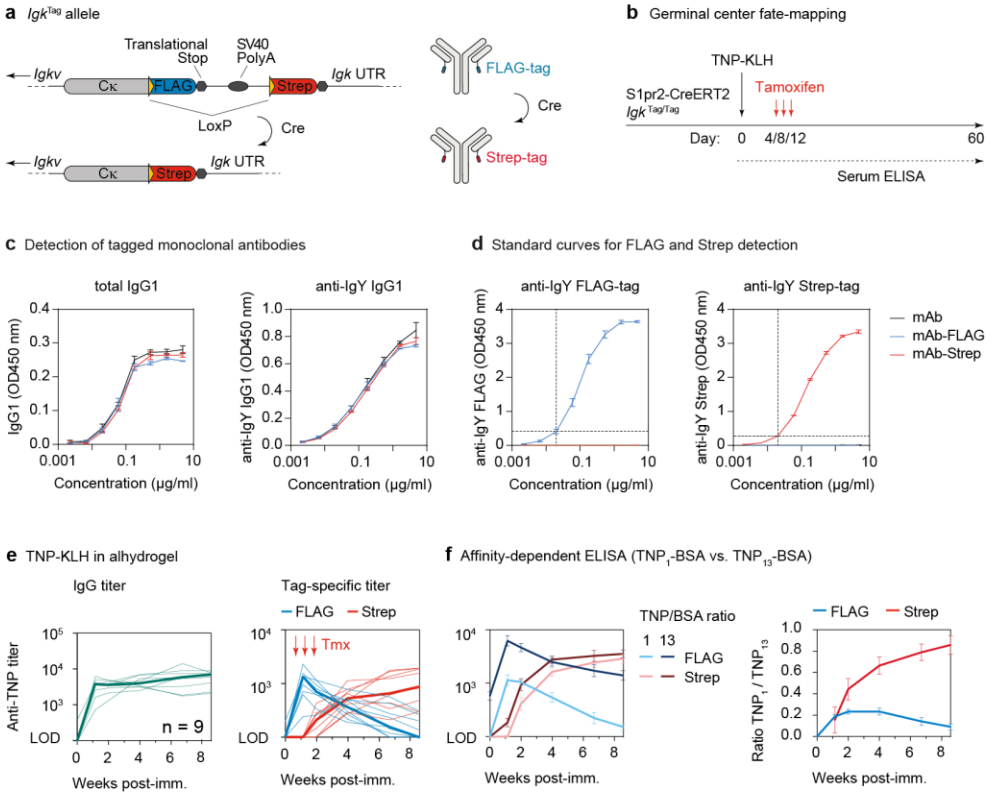

Figure 6: GC-derived antibodies are efficiently fate-mapped in Igκ-tag mice. *(a) Schematic representation of the Igκ^{Tag} allele before and after cre-mediated recombination. (b) Overview of the setup used to fate-map the BCR of GC B cells and their progenitors. (c) ELISA detection of total IgG1 and IgY-binding IgG1 for monoclonal antibodies modified with a FLAG- or Strep-tag. Error bars represent the SD of three independent titration curves. (d) ELISA detection of FLAG and Strep on tagged monoclonal antibodies. The OD450 nm value at an antibody concentration of 20 ng/ml (indicated by the dotted line) was used to calculate endpoint titers in serum samples. (e) Anti-TNP total IgG and tag-specific endpoint titers in mice immunized i.p. with TNP-KLH absorbed in alhydrogel adjuvant. Thin lines represent individual mice and thick lines the medians of the log-transformed endpoint titers. Results are from 9 mice from 2 independent experiments. (f) Relative affinity of anti-TNP FLAG- and Strep-tagged antibodies as estimated by ELISA using TNP(1)-BSA or TNP(13)-BSA as capture reagent. The right panel shows the ratio between anti-TNP(1)-BSA and anti-TNP(13)-BSA titers that was calculated per sample. Lines show the means of the log-transformed endpoint titers and error bars represent the SEM.*

B cells derived from recall GCs contribute little to antibody levels

To determine the contribution of primary-derived antibodies to recall antibody responses, we used Igκ-tag mice for prime-boost experiments. By giving tamoxifen during the first immune response, only antibodies produced by memory B cells and plasma cells derived from primary GCs will be Strep-tagged. Since there is little re-entry of memory B cells into secondary GCs (14), recall GC responses will primarily generate FLAG-tagged antibodies. First, we used a prime-boost model with TNP-KLH in alum, boosting one and two months after primary immunization (**Figure 7a**). As expected, TNP titers increased upon boosting, seen by both IgG and Igκ detection (**Figure 7b**). FLAG-tagged antibodies were produced after both boosts, but were short-lasting and decreased again below the limit of detection (**Figure 7b**). Strep-tagged antibodies also increased after boosting and remained more stable, indicating that elevated IgG and Igκ titers upon boosting mainly consist of primary-derived antibodies (**Figure 7b**). To quantify this, we calculated a 'primary addiction index' with the percentage of Strep+ titer over the total (FLAG+ and Strep+) titer.

Although a high primary addiction index was expected in the secondary response due to MBC responses, secondary GCs could potentially generate new MBCs that participate in tertiary responses. However, even after the second boost, more than 95% of the total TNP titer was composed of primary-derived antibodies (**Figure 7c**). To prove that FLAG-tagged antibodies produced after boosting are mainly formed by extrafollicular responses, IgM was depleted from serum samples collected one week after each boost (**Figure 7d**). While IgM depletion did not affect Strep-tagged titers, FLAG-tagged titers were significantly reduced in IgM-depleted serum (**Figure 7e**), supporting the idea that FLAG-tagged titers are largely generated by extrafollicular plasma cells.

Next, we investigated if primary addiction was also seen in the more relevant setting of complex protein immunization and in response to variant antigen. Since most people have been infected with influenza before they are vaccinated, mice were first primed by intranasal infection with influenza strain PR8. After 3 months, when extrafollicular FLAG-tagged antibodies had largely disappeared, and after 4 months, mice were homologously or heterologously boosted with HA_{P8} or HA_{FM1} protein, respectively (**Figure 7f**). In homologously boosted mice, both HA_{P8} boosts resulted in an increase of HA_{P8}-binding Strep-tagged antibodies (**Figure 7g**). New FLAG-tagged antibodies were also formed, but total titers were still primarily composed of Strep-tagged antibodies (**Figure 7g**). PR8 infection also resulted in some generation of FM1 cross-reactive Strep-tagged antibodies, which increased slightly upon heterologous boosting with HA_{FM1} (**Figure 7h**). New FLAG-tagged HA_{FM1} binding antibodies were also generated, resulting in a marked decrease in primary addiction after two boosts. This indicates that recall GCs are useful for generating memory against variant antigen.

Lastly, we used Igκ-tag mice to study the contribution of recall immune responses to antibody levels upon immunization with SARS-CoV-2 Spike mRNA-LNPs, which produced high-quality recall GCs (**Figure 5c**). Total IgG and Igκ antibody titers against the receptor-binding domain (RBD) of the Spike protein could be detected after primary immunization, increased after the first boost, and stayed relatively stable after the second boost (**Figure 7i**). The primary response mainly consisted of extrafollicular FLAG-tagged antibodies, as GC-derived Strep-tagged antibodies could barely be detected (**Figure 7i**). However, Strep-tagged titers increased markedly upon boosting, indicating that memory B cells had been potently formed (**Figure 7i**). No FLAG-tagged antibodies were detected after the first boost, but some new antibody formation was seen after the second boost. However, there was clear suppression of antibody generation by recall GCs, as these titers were much lower than the Strep-tagged titers in the secondary response, which were generated by memory B cells derived from primary GCs. In conclusion, we show that antibodies derived from recall GCs contribute little to serum antibody titers upon homologous boosting.

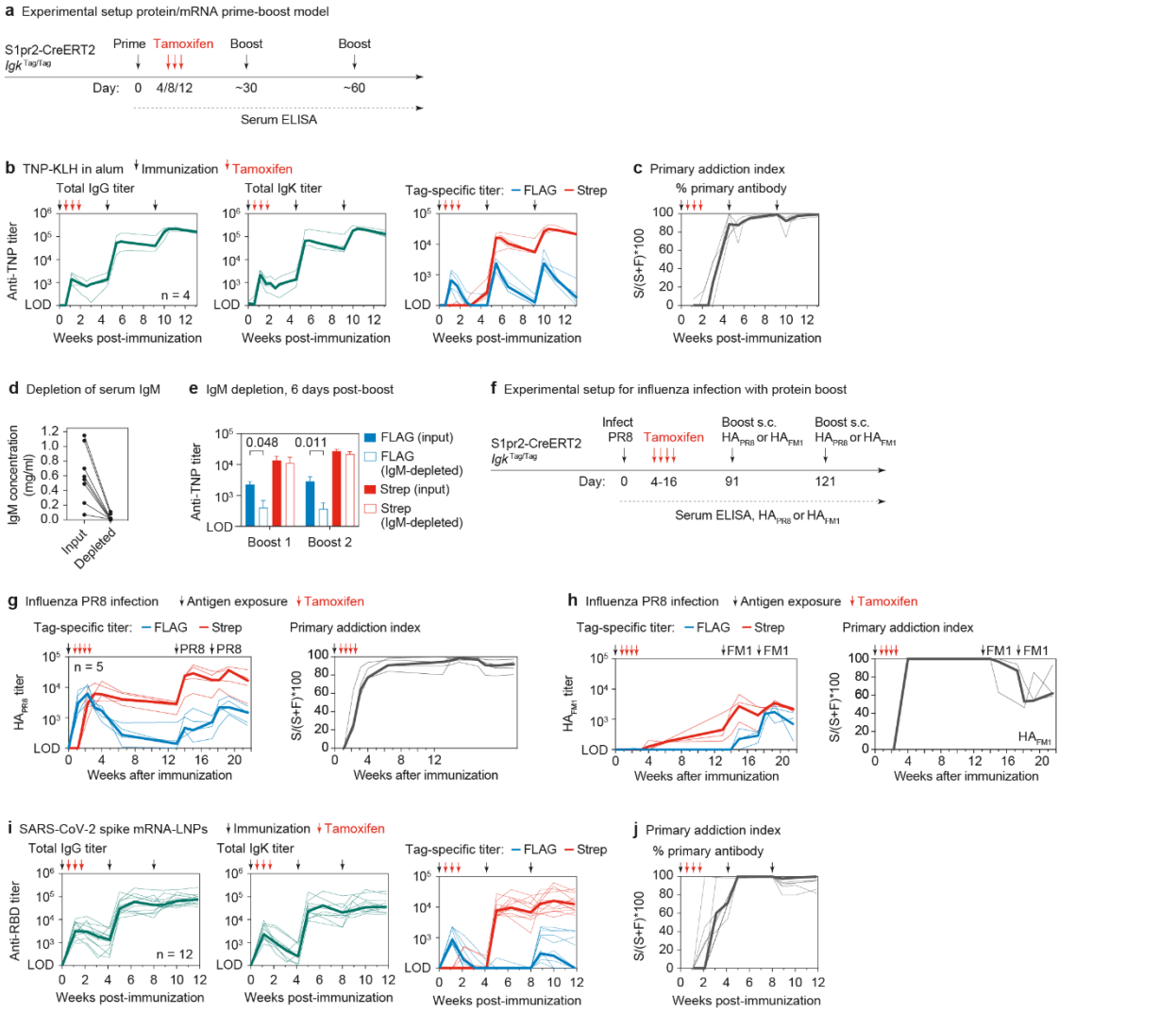

Figure 7: B cells derived from recall GCs contribute little to antibody levels. *(a) Schematic representation of the experimental setup to measure the contribution of primary- and recall-derived GC B cells to antibody levels. (b) Detection of anti-TNP IgG (left panel), Igκ (middle panel), and tag-specific titers (right panel) by ELISA in serum samples from mice immunized with TNP-KLH. Results are from 4 mice from 2 independent experiments. Thin lines represent individual mice and thick lines the medians of the log-transformed endpoint titers. (c) The percentage of anti-TNP antibody titer that was derived from primary GC B cells (the "primary addiction index") was calculated by dividing the Strep+ titer by the total (FLAG+ and Strep+) titer of each sample, multiplied by 100 (S/(S+F)*100). Thin lines represent individual mice and thick lines the median. (d) Total IgM concentrations in serum samples collected 6 days after the first or second boost before and after depletion of IgM by immunoprecipitation, as measured by ELISA. (e) Tag-specific anti-TNP titers before and after IgM depletion. Bars show the means of the log-transformed titers and error bars represent the SEM. P-values are for paired T-tests, only showing statistically significant ($p < 0.05$) values. (f) Schematic representation of influenza infection and HA protein boosting strategy. S1pr2-Igk$^{Tag/Tag}$ mice were intranasally infected with influenza strain PR8 and boosted subcutaneously (s.c.) with HA_{PR8} or HA_{FM1} in alhydrogel. (g) Anti-HA_{PR8} FLAG- and Strep-tagged titers in mice that were homologously boosted with HA_{PR8} (left panel) and quantification of the primary addiction index calculated as in (c) (right panel). (h) Anti-HA_{FM1} FLAG- and Strep-tagged titers in mice that were heterologously boosted with HA_{FM1} (left panel) and quantification of the primary addiction index calculated as in (c) (right panel). (i) Detection of anti-WH1 RBD IgG (left panel), Igκ (middle panel), and tag-specific titers (right panel) by ELISA in serum samples from mice immunized with WH1 Spike mRNA-LNPs. Results are from 12 mice from 3 independent experiments. (j) Primary addiction index calculated as in (c).*

Discussion

Here, we show that antibodies derived from primary immune responses suppress the quality of recall GCs upon re-exposure to the same antigen. When immunizing with HA protein, prior exposure to the same antigen did not reduce the total number of B cells that was recruited to GCs, but recall GC B cells showed less antigen-binding compared to primary GC B cells. As we also measured a high proportion of non-binding B cells in primary GCs, the nature of these cells has yet to be determined. High numbers of GC B cells that do not show measurable antigen-binding have also been observed by others (47,48). One explanation could be that these cells are specific for the immunogen, but are too low-affinity to be detected with conventional methods (18,47). Alternatively, these cells might be specific for neo-epitopes in modified, non-native forms of immunogen that are only generated in *in vivo*, also known as 'dark antigen' (47). In the latter case, antibodies derived from these B cells might still be useful if the same neo-epitopes are formed during infection.

By using hapten-carriers, we showed that prior B cell responses inhibit B cell recruitment to recall GCs, but this is overcome by the presence of T cell memory. In absence of T cell memory, when mice were boosted with hapten conjugated to a different carrier protein than for primary immunization, GC formation and plasma cell generation were inhibited. However, when the same carrier protein was used for priming and boosting, naive B cells were efficiently recruited to GCs, although they showed less antigen-binding than primary GC B cells. These data indicate indicate that previous B cell responses impair activation of naïve B cells, at least during epitope-focused responses to haptens. In presence of T cell memory, increased T cell help might allow recruitment of naive B cells with lower affinity for the immunogen, resulting in larger but low-quality GCs.

Multiple studies have shown that passive administration of antigen-specific serum or monoclonal antibodies can inhibit GC responses and antibody production (35,37,38). We show that inhibition of plasma cell generation, and therefore antibody production, during the primary response increased recall GC quality. These results indicate that antibodies derived from primary immune responses are responsible for the suppression of GC quality. In absence of T cell memory, inhibition of plasma cell formation increased B cell recruitment to recall GCs, although GCs were still smaller in size than primary GCs. However, the formation of antigen-specific antibodies was not fully prevented in this model and since hapten responses are essentially focused on a single epitope, it is likely that remaining antibodies could still inhibit B cell activation. In response to HA_{PR8} immunization, inhibition of plasma cell formation by primary GCs increased the number of recall GC B cells that showed detectable binding to antigen, again indicating that pre-existing antibodies are responsible for suppressed recall GC quality.

Two possible mechanisms could explain why antibodies suppress recall immune responses. First, antibodies can mask antigenic epitopes, preventing recognition by naive B cells. Second, antigen-specific antibodies can promote Fc-dependent antigen clearance, limiting antigen availability (34–36). Both mechanisms could cause reduced B cell activation, inhibiting B cell recruitment to recall GCs. Masking of epitopes that are recognized by primary antibodies could also cause a shift in epitope specificity by preferential recruitment of naive B cells recognizing different epitopes, which might show less measurable binding to the immunogen. A change in the specificity of B cells recruited to primary and recall GCs is supported by the observation that upon NP-carrier immunization, while primary responses are characterized by the recruitment of Igλ-expressing B cells, fewer Igλ-expressing B cells were found in recall GCs compared to primary GCs. This indicates that there is a shift from Igλ to Igκ usage upon secondary NP

immunization, which has also been observed in other studies (49). Although the generation of high-quality recall GCs seems preferable, epitope masking could be a useful process when it leads to the generation of antibodies against new or different, non-immunodominant epitopes. The generation of a diverse repertoire of antibodies and memory cells is beneficial, as it increases the chance of having cross-reactive antibodies against new viral variants. Epitope masking could also explain why heterologous boosting can partially overcome antibody-mediated suppression, as naïve B cells recognizing new viral epitopes could be recruited to GCs.

Interestingly, when immunizing with mRNA-LNPs, recall GC B cells showed similar antigen-binding compared to primary GC B cells. A possible explanation for the higher quality of mRNA-induced recall GCs is more sustained production of antigen by mRNA immunization. Previous studies have shown that administration of excess antigen or sequential antigen administration can overcome the suppressive effect of antigen-specific antibodies (22,37,50). Therefore, mRNA vaccination could help to recruit more high-affinity naive B cells to recall GCs by producing enough antigen to overcome antibody-mediated suppression.

Lastly, we used a novel molecular fate-mapping system to measure the contribution of recall GC reactions to serum antibody levels. This revealed that B cells derived from recall GCs contribute little to antibody titers. Although homologous booster immunizations generate much higher levels of antigen-specific antibodies, the great majority is derived from B cells that were engaged in the primary GC responses. In most cases, this correlates with the low quality of recall GCs we observed. Heterologous boosting with HA protein increased the relative contribution of recall GC responses to antibody levels, showing that recall GCs are useful for producing antibodies against variant antigen. However, directly comparing the contribution of *de novo* immune responses upon heterologous boosting to homologous boosting or primary responses requires a similar setup as in our GC experiments, in which all mice are boosted with HA_{PR8} but primed with the either irrelevant protein, HA_{PR8} or HA_{FM1}. Surprisingly, although recall GCs induced by Spike mRNA immunization were high-quality, they only generated low titers of RBD-specific antibodies. Recall GCs also did not generate high titers against full Spike protein (data shown in (45)), indicating that the difference cannot be explained by a shift to non-RBD epitopes. One explanation could be that GC B cells show detectable binding by flow cytometry, but still have lower affinity than primary GC B cells. A previous study showed that administration of monoclonal antibodies specific for two immunodominant epitopes of Spike RBD generated low-affinity MBCs that recognized different epitopes, not resulting in neutralization of the virus (51). However, in contrast to our results, they did not show a significant reduction in the formation of antigen-specific antibodies.

Importantly, impaired antibody production by recall GCs does not have to be detrimental, especially when boosting with the same or closely related antigens, as MBC responses could generate sufficiently high antibody titers. However, the induction of high-quality recall GCs can be desired to generate antibodies against new or non-immunodominant epitopes. Although we show that antibodies formed during primary immune responses suppress germinal center quality, they might also cause a shift in antibody responses to novel epitopes. More research is needed to determine to what extent recall GC B cells are aimed at such novel epitopes. Together, these insights into the mechanisms behind recall GC quality could be used to optimize prime-boost vaccination strategies.

Methods

Mice

Wild-type C57BL/6J, *Rosa26*$^{Confetti/Confetti}$ (52) and *Prdm1*$^{flox/flox}$ mice (53) were obtained from The Jackson Laboratory. *Aicda*^{CreERT2} mice (54) were a kind gift from Jean-Claude Weill and Claude-Agne`s Reynaud (Université Paris-Descartes). *S1pr2*^{CreERT2} BAC-transgenic mice (46) were kindly provided by T. Kurosaki and T. Okada (U. Osaka, RIKEN-Yokohama). *Igκ*^{Tag} mice were generated at the Rockefeller University as described previously (45). In short, the gene encoding the immunoglobulin kappa (Igκ) light chain was engineered with a C-terminal LoxP-flanked FLAG-tag (DYKDDDDK) and downstream Strep-II tag (WSHPQFEK). All mice were held at the immunocore clean facility at the Rockefeller University under specific pathogen-free conditions. All mouse procedures were approved by the Rockefeller University's Institutional Animal Care and Use Committee.

Immunizations, infections, and treatments

Immune responses were induced in 7- to 12-week-old mice by subcutaneous immunization in the footpad, intraperitoneal immunization, intramuscular immunization in the quadricep muscles, or intranasal infection as given in table 1. Antigens were supplemented with 1/3 volume of aluminum hydroxide gel (alhydrogel, Invivogen) or Imject^{TM} alum (ThermoScientific). In *Igκ*^{Tag} mice, antibodies of GC B cells and progenitors were fate-mapped by oral gavage of 10 mg tamoxifen (Sigma) dissolved in 200 µl corn oil at day 4, 8 and 12 post primary immunization. In *Prdm1*$^{flox/flox}$ mice, plasma cell generation was inhibited during the primary immune response by giving tamoxifen at day 3, 6, 9 and 12 post immunization. Blood samples were drawn by cheek puncture and collected into microtubes prepared with clotting activator serum gel (Sarstedt, #41.1378.005).

Table 1: antigen, mRNA and pathogen used for immunization or infection

Antigen	Source	Route of administration	Dose	Adjuvant
CGG	Biosearch Technologies (#C-1000)	Subcutaneous footpad	10 µg	Alhydrogel
HA_{PR8}	Homemade (see below)	Subcutaneous footpad	20 µg	Alhydrogel
HA_{FM1}	Homemade (see below)	Subcutaneous footpad	20 µg	Alhydrogel
NP(24)-CGG	Biosearch Technologies (#N-5055C)	Subcutaneous footpad	10 µg	Alhydrogel
NP-OVA	Biosearch Technologies (#N-5051)	Subcutaneous footpad	10 µg	Alhydrogel
OVA	Biosearch Technologies (O-1000)	Subcutaneous footpad	10 µg	Alhydrogel
TNP(17)-KLH	Biosearch Technologies (#T-5060)	Intraperitoneal	50 µg	Alhydrogel / Alum
mRNA	Source	Route of administration	Dose	
HA_{PR8} mRNA-LNP	Produced as described in (45)	Intramuscular quadricep muscles	3 µg	
Luc mRNA-LNP	Produced as described in (45)	Intramuscular quadricep muscles	3 µg	
WH1 Spike mRNA-LNP	Produced as described in (45)	Intramuscular quadricep muscles	3 µg	
Pathogen	Source	Route of administration	Dose	
PR8 influenza virus	Provided by M. Carroll, Harvard University Medical School	Intranasal infection	~33 PFU	

Protein production

Recombinant HA_{PR8} and HA_{FM1} proteins used for immunizations and ELISAs were produced in-house in suspension-adapted Chinese hamster ovary (CHO-DG44) cells, following the same procedure as described previously (14). The coding sequences for A/Puerto Rico/8/1934 (PR8) and A/Fort Monmouth/1/1947 (FM1) were followed by a C-terminal thrombin cleavage site, foldon domain for trimerization, AviTag for biotinylation and His-tag for purification with Ni-Sepharose excel resin (GE Healthcare). Cysteine residues were introduced into the HA sequence to create trimer-stabilizing disulfide bonds (55). For immunizations, the C-terminal domains not native to HA (foldon, Avi-tag and His-tag) were removed by thrombin cleavage. For ELISAs, proteins were not treated with thrombin. HA proteins were subsequently FPLC-purified and stored in PBS. For flow cytometry, biotinylated HA proteins were generated with the Y98F mutation, preventing sialic acid binding (14).

To produce standards for the detection of FLAG- or Strep-tagged antibodies in serum, a high-affinity IgY-specific monoclonal antibody (mAb) obtained from CGG-immunized mice (clone 2.1 (56)) was modified with a FLAG- or Strep-tag. Heavy and light chain constant regions in the original human antibody plasmids (57) were replaced with mouse IgG1 and Igκ constant regions. The C-terminus of C_κ was modified to encode a LoxP site and Ser-Gly-Gly linker followed by either a FLAG or Strep-tag. The mAb-FLAG or mAb-Strep light chain plasmids were transfected together with the heavy chain plasmid into 293F cells and purified using protein-G affinity chromatography as described before (56).

To look at affinity maturation of FLAG- and Strep-tagged anti-TNP antibody titers, custom low and high ratio TNP-BSA conjugates were made in-house. TNP-ε-Aminocaproyl-OSu (Biosearch Technologies #T-1030) was incubated at a molar ratio of either 1:2 or 1:20 with 2.5 mg/ml (75 µM) BSA (ThermoScientific #77110) in PBS with 20% DMSO for 2 hours at room temperature (RT) while rotating, protected from light. Insoluble material was spun down by centrifugation at 500 xG for 5 minutes. Unconjugated TNP-ε-Aminocaproyl-OSu was removed by dialysis in PBS. Final TNP and BSA concentrations were determined by measuring absorbance at 280 nm and 348 nm, using the extinction coefficients of BSA and TNP at both wavelengths. Final TNP:BSA conjugation ratios were estimated to be ~1:1 and ~1:13.

Flow cytometry

For flow cytometry, popliteal (after footpad immunization) or inguinal (after intramuscular immunization) lymph nodes were collected and mechanically disassociated with disposable micropestles (Axygen). Cells were resuspended in PBS supplemented with 0.5% BSA and 1 mM EDTA and stained with fluorescently-labeled antibodies (table 2) for 30 minutes on ice. Fluorescently labeled antigen tetramers were generated by incubating biotinylated HA (see above) or SARS-CoV-2 Spike RBD-His protein (Sino Biological, #40592-V08B-B) with BV421-labeled streptavidin for 30 min at RT at a molar ratio of 4:1. Before analysis, samples were washed in PBS supplemented with 0.5% BSA and 1 mM EDTA and filtered. Samples were analyzed on a BD FACS Symphony cytometer or BD FACS Diva 9.5 for cell sorting.

Table 2: flow cytometry reagents

Reagent	Clone	Fluorophore	Final dilution	Source	Catalog number
Anti-B220	RA3-6B2	BV785	1:400	BioLegend	#103246
Anti-CD138	281-2	BV650	1:400	BioLegend	#142517
Anti-CD38	90	APC	1:400	eBioscience	#17-0381-82
Anti-Fas/CD95	Jo2	PE/Cy7	1:800	BD Biosciences	#557653
Anti-IgD	11-26c.2a	PE	1:200	BioLegend	#405705
Anti-Igλ	R26-46	FITC	1:200	BD Biosciences	#553434
Anti-TCRβ	H57-697	APC/eFluor780	1:400	eBioscience	#47-5961-82
GL7	GL7	FITC	1:200	BD Biosciences	#553666
NP(16)-PE	N/A	PE	1:200	Biosearch Technologies	#N-5070
Streptavidin	N/A	BV421	1:200	BioLegend	#405226

Single-cell Nojima cultures

NB-21 cells were cultured in DMEM supplemented with 10% heat-inactivated FBS and penicillin streptomycin solution (Corning). One day before single-cell sorting, NB-21 cells were detached and resuspended in OptiMEM, irradiated (20 Gy) and seeded into 96-well plates at 3,000 cells per well in OptiMEM supplemented with 10% heat-inactivated FBS, 2 mM L-glutamine, 1 mM sodium pyruvate, 50 µM 2-ME, penicillin streptomycin solution, 10 mM HEPES, MEM vitamin solution (Sigma) and MEM non-essential amino acids (Gibco). The following day, single GC B cells were sorted into wells and 150 µl of supplemented OptiMEM along with 30 µg/ml LPS (Sigma-Aldrich, #L6511) and 4 ng/ml IL-4 (Fisher Scientific, #404-ML) was added to each well. 7 days after sorting, supernatants were screened for Ig production by ELISA and Ig-positive wells (OD450 nm value above 0.15) were selected.

ELISA

96-well high-binding half-area microplates (Greiner or Corning) were coated overnight at 4°C with antigen or capture antibody (1 µg /ml) in PBS (25 µl per well). Antigens and antibodies used for ELISAs are shown in table 3. In between each step, plates were washed with PBS + 0.05% Tween20 (PBS-Tween). After overnight incubation, plates were blocked with 2.5% bovine serum albumin (BSA, Sigma) in PBS for 2 hours at RT. Serum samples were diluted 1:100 in PBS-Tween and titrated in 3-fold dilutions. When FLAG- and Strep-tagged antibodies were detected in serum, ELISAs were performed side by side and with internal standards on each 96-well plate. Mouse anti-IgY mAb-FLAG or mAb-Strep were also serially titrated in 3-fold dilutions. Plates were incubated with sample for 2 hours at RT, followed by incubation with detection antibody for 30-45 minutes at RT. Dilutions of anti-FLAG and anti-Strep antibodies were defined so that the curves generated by titration of FLAG- and Strep-tagged mAbs were equivalent. To develop ELISAs, plates were incubated with 3,3’,5,5’-tetramethylbenzidine substrate (slow kinetic form, Sigma) and the reaction was stopped with 1N hydrochloric acid. Optical Density (OD) absorbance was measured at 450 nm on a Fisher Scientific accuSkan FC plate reader. To normalize FLAG and Strep endpoint titers, the serum titer dilution was calculated at which each sample passed the threshold OD value of its respective mAb at a fixed concentration of either 20 or 6.67 ng/µl. Titers were calculated by logarithmic interpolation of the dilutions with readings immediately above and immediately below the mAb OD450 nm value used (58).

Table 3: ELISA reagents

Capture reagents	Source	Final concentration	Catalog number
Chicken IgY	Gallus Immunotech	10 µg/ml	#IgY-100
Goat anti-mouse Ig	Southern Biotech	1 µg/ml	#5300-05B
Goat anti-mouse IgG1	Southern Biotech	1 µg/ml	#1073-01
Goat anti-mouse IgM	Southern Biotech	1 µg/ml	#1020-01
HA_{PR8}	See above	1 µg/ml	N/A
NP(1-4)-BSA	Biosearch Technologies	10 µg/ml	#N-5050XL
SARS-CoV-2 Wuhan-Hu-1 Spike RBD	Provided by P. Wilson	1 µg/ml	N/A
TNP(1)-BSA	Homemade (see above)	2 µg/ml	N/A
TNP(13)-BSA	Homemade (see above)	2 µg/ml	N/A
TNP(4)-BSA	Biosearch Technologies	10 µg/ml	#T-5050
HRP-labeled detection antibodies	Source	Final dilution	
Goat anti-mouse Ig	Southern Biotech	1:2,000	#1010-05
Goat anti-mouse IgG	Jackson Immunoresearch	1:10,000	#15-035-071
Goat anti-mouse IgG1	Southern Biotech	1:10,000	#1070-05
Goat anti-mouse IgM	Southern Biotech	1:5,000	#5300-05B
Mouse anti-Strep (clone Strep-tag II StrepMAB-Classic)	Bio-Rad	1:2,500-4,500	#MCA2489P
Rat anti-mouse Igκ	Abcam	1:10,000	#ab99632
Rabbit anti-FLAG-HRP (clone D6W5B)	Cell Signaling Technology	1:1,500	#86861S

To deplete IgM from serum samples, anti-mouse IgM agarose beads (Sigma #A4540) were used according to instructions from the manufacturer. Beads were washed with PBS and samples were incubated at a ratio of 1:20 sample to beads overnight at 4°C while rotating. The bead-bound IgM fraction was removed by centrifugation for 3 minutes at 10,000 G and the supernatant was collected for subsequent ELISAs. IgM concentrations were interpolated using an IgM standard (Southern Biotech, #5300-01B).

Statistical analysis and software

Flow cytometry analysis was performed using FlowJo v.10 software. Graphs were made in GraphPad Prism v.9 and edited in Adobe Illustrator CS. Statistical analysis was performed using GraphPad Prism v.9 as indicated in figure legends. For data plotted on logarithmic scales, statistical analysis was performed on the log-transformed data. ELISA samples with absorbance values below the limit of detection were assigned a value of 100, as the top dilution was 1:100.

Supplementary figures

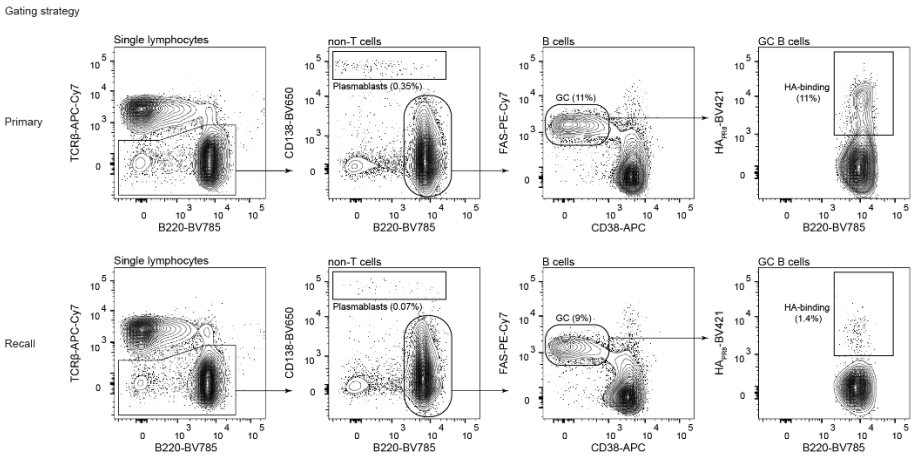

Supplementary Figure 1: general flow cytometry gating strategy. *General gating strategy to identify plasma cells, GC B cells and antigen-binding GC B cells. Plots show examples for primary and recall GCs induced by HA_{PR8} immunization as shown in Figure 2a. Single lymphocytes were gated based on forward and side scatter.*

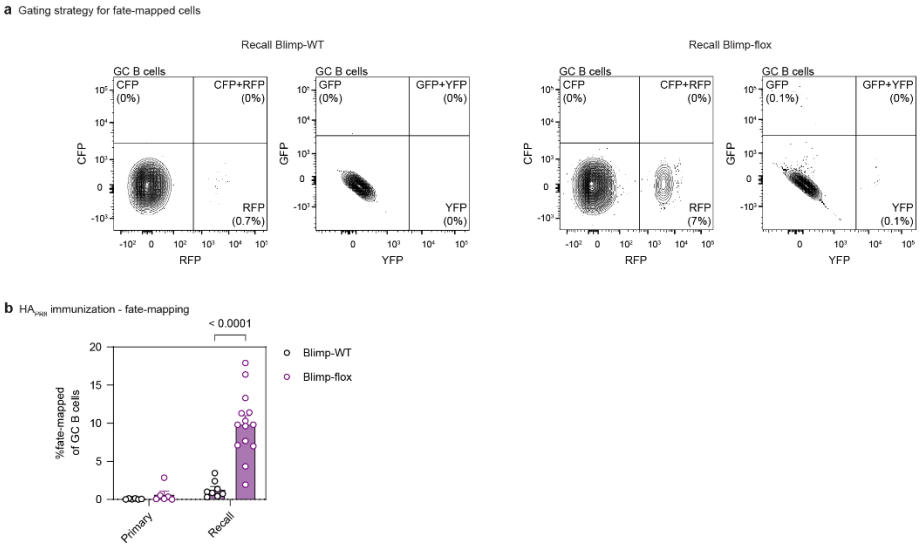

Supplementary Figure 2: fate-mapping of primary GC B cells. *(a) Gating strategy to identify fate-mapped GC B cells in AID-confetti mice, related to Figure 3. (b) Memory re-entry in primary and recall GCs induced by HA_{PR8} immunization in Blimp-flox and Blimp-WT mice as shown in Figure 3a.*

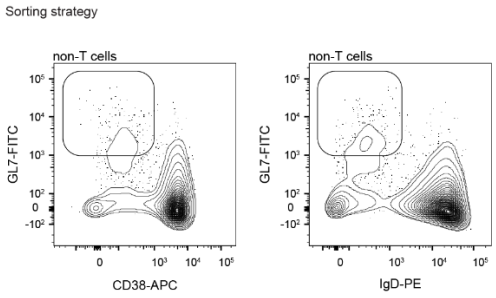

Supplementary Figure 3: sorting strategy. *Gating strategy for sorting of GC B cells for single-cell Nojima cultures, related to Figure 4.*

References

1. Victora GD, Nussenzweig MC. Germinal Centers. Annu Rev Immunol. 2022;40:413–42.
2. Schwickert TA, Victora GD, Fooksman DR, Kamphorst AO, Mugnier MR, Gitlin AD, et al. A dynamic T cell-limited checkpoint regulates affinity-dependent B cell entry into the germinal center. Journal of Experimental Medicine. 2011;208(6):1243–52.
3. Yeh CH, Nojima T, Kuraoka M, Kelsoe G. Germinal center entry not selection of B cells is controlled by peptide-MHCII complex density. Nat Commun. 2018;9(1):1–11.
4. Elsner RA, Shlomchik MJ. Germinal Center and Extrafollicular B Cell Responses in Vaccination, Immunity, and Autoimmunity. Immunity. 2020;53(6):1136–50.
5. Muramatsu M, Kinoshita K, Fagarasan S, Yamada S, Shinkai Y, Honjo T. Class switch recombination and hypermutation require activation-induced cytidine deaminase (AID), a potential RNA editing enzyme. Cell. 2000;102(5):553–63.
6. Pavri R, Nussenzweig MC. AID Targeting in Antibody Diversity. Adv Immunol. 2011;110:1–26.
7. Roco JA, Mesin L, Binder SC, Nefzger C, Gonzalez-Figueroa P, Canete PF, et al. Class-Switch Recombination Occurs Infrequently in Germinal Centers. Immunity. 2019;51(2):337-350.
8. Tunyaplin C, Shaffer AL, Angelin-Duclos CD, Yu X, Staudt LM, Calame KL. Direct Repression of prdm1 by Bcl-6 Inhibits Plasmacytic Differentiation. The Journal of Immunology. 2004;173(2):1158–65.
9. Inoue T, Moran I, Shinnakasu R, Phan TG, Kurosaki T. Generation of memory B cells and their reactivation. Immunol Rev. 2018;283(1):138–49.
10. Weisel FJ, Zuccarino-Catania G v., Chikina M, Shlomchik MJ. A Temporal Switch in the Germinal Center Determines Differential Output of Memory B and Plasma Cells. Immunity. 2016;44(1):116–30.
11. Weisel F, Shlomchik M. Memory B Cells of Mice and Humans. Annu Rev Immunol. 2017;35:255–84.
12. Kurosaki T, Kometani K, Ise W. Memory B cells. Nat Rev Immunol. 2015;15(3):149–59.
13. Viant C, Weymar GHJ, Escolano A, Chen S, Hartweger H, Cipolla M, et al. Antibody Affinity Shapes the Choice between Memory and Germinal Center B Cell Fates. Cell. 2020;183(5):1298-1311.
14. Mesin L, Schiepers A, Ersching J, Barbulescu A, Cavazzoni CB, Angelini A, et al. Restricted Clonality and Limited Germinal Center Reentry Characterize Memory B Cell Reactivation by Boosting. Cell. 2020;180(1):92-106.
15. Monto AS, Malosh RE, Petrie JG, Martin ET. The Doctrine of Original Antigenic Sin: Separating Good From Evil. J Infect Dis. 2017;215(12):1782–8.
16. Cobey S, Hensley SE. Immune history and influenza virus susceptibility. Curr Opin Virol. 2017;22:105.

17. Zhang A, Stacey HD, Mullarkey CE, Miller MS. Original Antigenic Sin: How First Exposure Shapes Lifelong Anti–Influenza Virus Immune Responses. The Journal of Immunology. 2019;202(2):335–40.

18. Yewdell JW, Santos JJS. Original Antigenic Sin: How Original? How Sinful? Cold Spring Harb Perspect Med. 2021;11(5):a038786.

19. Francis T. On the Doctrine of Original Antigenic Sin. Proc Am Philos Soc. 1960;104(6):572–8.

20. Gostic KM, Ambrose M, Worobey M, Lloyd-Smith JO. Potent protection against H5N1 and H7N9 influenza via childhood hemagglutinin imprinting. Science. 2016;354(6313):722–6.

21. Fazekas de St Groth, Webster RG. Disquisitions on Original Antigenic Sin I. Evidence in Man. Journal of Experimental Medicine. 1966;124(3):331–45.

22. Fazekas S, St DX, Groth MD, Webster RG. Disquisitions on Original Antigenic Sin II. Proof in Lower Creatures. Journal of Experimental Medicine. 1966;124(3):347–61.

23. Wheatley AK, Fox A, Tan HX, Juno JA, Davenport MP, Subbarao K, et al. Immune imprinting and SARS-CoV-2 vaccine design. Trends Immunol. 2021;42(11):956–9.

24. Reynolds CJ, Pade C, Gibbons JM, Otter AD, Lin K-M, Muñoz Sandoval D, et al. Immune boosting by B.1.1.529 (Omicron) depends on previous SARS-CoV-2 exposure. Science. 2022;377(6603).

25. Röltgen K, Nielsen SCA, Silva O, Younes SF, Zaslavsky M, Costales C, et al. Immune imprinting, breadth of variant recognition, and germinal center response in human SARS-CoV-2 infection and vaccination. Cell. 2022;185(6):1025-1040.

26. Aydillo T, Rombauts A, Stadlbauer D, Aslam S, Abelenda-Alonso G, Escalera A, et al. Immunological imprinting of the antibody response in COVID-19 patients. Nat Commun. 2021;12(1):1–13.

27. Kim JH, Skountzou I, Compans R, Jacob J. Original Antigenic Sin Responses to Influenza Viruses. J Immunol. 2009;183(5):3294.

28. Tangye SG, Avery DT, Deenick EK, Hodgkin PD. Intrinsic Differences in the Proliferation of Naive and Memory Human B Cells as a Mechanism for Enhanced Secondary Immune Responses. The Journal of Immunology. 2003;170(2):686–94.

29. Heyman B. Regulation of Antibody Responses via Antibodies, Complement, and Fc Receptors. Annu Rev Immunol. 2003;18:709–37.

30. Heyman B. Antibodies as natural adjuvants. Curr Top Microbiol Immunol. 2014;382:201–19.

31. Batista FD, Harwood NE. The who, how and where of antigen presentation to B cells. Nat Rev Immunol. 2009;9(1):15–27.

32. Phan TG, Green JA, Xu Y, Cyster JG. Immune complex relay by subcapsular sinus macrophages and noncognate B cells drives antibody affinity maturation. Nat Immunol. 2009;10(7):786–93.

33. Smith T. Active immunity produced by so called balanced or neutral mixtures of diphteria toxin and antitoxin. Journal of Experimental Medicine. 1909;11(2):241–56.

34. Zarnitsyna VI, Ellebedy AH, Davis C, Jacob J, Ahmed R, Antia R. Masking of antigenic epitopes by antibodies shapes the humoral immune response to influenza. Philosophical Transactions of the Royal Society B: Biological Sciences. 2015;370(1676).

35. Bergström JJE, Xu H, Heyman B. Epitope-specific suppression of IgG responses by passively administered specific IgG: Evidence of epitope masking. Front Immunol. 2017;8(MAR):238.

36. Na D, Kim D, Lee D. Mathematical modeling of humoral immune response suppression by passively administered antibodies in mice. J Theor Biol. 2006;241(4):830–51.

37. Tas JMJ, Koo J-H, Lin Y-C, Xie Z, Steichen JM, Jackson AM, et al. Antibodies from primary humoral responses modulate recruitment of naive B cells during secondary responses. Immunity. 2022;55(10):1856–71.

38. Pape KA, Taylor JJ, Maul RW, Gearhart PJ, Jenkins MK. Different B cell populations mediate early and late memory during an endogenous immune response. Science. 2011;331(6021):1203–7.

39. Yoshino T, Kondo E, Cao L, Takahashi K, Hayashi K, Nomura S, et al. Inverse Expression of bcl-2 Protein and Fas Antigen in Lymphoblasts in Peripheral Lymph Nodes and Activated Peripheral Blood T and B Lymphocytes. Blood. 1994;83(7):1856–61.

40. Oliver AM, Martin F, Kearney JF. Mouse CD38 is down-regulated on germinal center B cells and mature plasma cells. The Journal of Immunology. 1997;158(3).

41. Nojima T, Haniuda K, Moutai T, Matsudaira M, Mizokawa S, Shiratori I, et al. In-vitro derived germinal centre B cells differentially generate memory B or plasma cells in vivo. Nat Commun. 2011;2(1):1–11.

42. Naito Y, Takematsu H, Koyama S, Miyake S, Yamamoto H, Fujinawa R, et al. Germinal Center Marker GL7 Probes Activation-Dependent Repression of N-Glycolylneuraminic Acid, a Sialic Acid Species Involved in the Negative Modulation of B-Cell Activation. Mol Cell Biol. 2007;27(8):3008.

43. Bhan AK, Nadler LM, Stashenko P, McCluskey RT, Schlossman SF. Stages of B cell differentiation in human lymphoid tissue. J Exp Med. 1981;154(3):737–49.

44. Hogan MJ, Pardi N. mRNA Vaccines in the COVID-19 Pandemic and Beyond. Annu Rev Med. 2022;73:17–39.

45. Schiepers A, Wout MFL van ’t, Greaney AJ, Zang T, Muramatsu H, Lin PJC, et al. Molecular fate-mapping of serum antibodies reveals the effects of antigenic imprinting on repeated immunization. bioRxiv. 2022.

46. Shinnakasu R, Inoue T, Kometani K, Moriyama S, Adachi Y, Nakayama M, et al. Regulated selection of germinal-center cells into the memory B cell compartment. Nat Immunol. 2016;17(7):861–9.

47. Finney J, Yeh C-H, Kelsoe | Garnett, Kuraoka M. Germinal center responses to complex antigens. Immunol Rev. 2018;284.

48. Kuraoka M, Schmidt AG, Nojima T, Feng F, Watanabe A, Kitamura D, et al. Complex Antigens Elicit Diverse Patterns of Clonal Selection in Germinal Centers. Immunity. 2016;44(3):542.

49. Reth M, Hämmerling GJ, Rajewsky K. Analysis of the repertoire of anti-NP antibodies in C57BL/6 mice by cell fusion. I. Characterization of antibody families in the primary and hyperimmune response. Eur J Immunol. 1978;8(6):393–400.

50. Tam HH, Melo MB, Kang M, Pelet JM, Ruda VM, Foley MH, et al. Sustained antigen availability during germinal center initiation enhances antibody responses to vaccination. Proc Natl Acad Sci U S A. 2016;113(43):E6639–48.

51. Schaefer-Babajew D, Wang Z, Muecksch F, Cho A, Raspe R, Johnson B, et al. Antibody feedback regulation of memory B cell development in SARS-CoV-2 mRNA vaccination. medRxiv. 2022.

52. Snippert HJ, van der Flier LG, Sato T, van Es JH, van den Born M, Kroon-Veenboer C, et al. Intestinal Crypt Homeostasis Results from Neutral Competition between Symmetrically Dividing Lgr5 Stem Cells. Cell. 2010;143(1):134–44.

53. Shapiro-Shelef M, Lin KI, McHeyzer-Williams LJ, Liao J, McHeyzer-Williams MG, Calame K. Blimp-1 is required for the formation of immunoglobulin secreting plasma cells and pre-plasma memory B cells. Immunity. 2003;19(4):607–20.

54. Dogan I, Bertocci B, Vilmont V, Delbos F, Mégret J, Storck S, et al. Multiple layers of B cell memory with different effector functions. Nature Immunology 2009 10:12. 2009;10(12):1292–9.

55. Lee PS, Zhu X, Yu W, Wilson IA. Design and Structure of an Engineered Disulfide-Stabilized Influenza Virus Hemagglutinin Trimer. J Virol. 2015;89(14):7417–20.

56. Tas JMJ, Mesin L, Pasqual G, Targ S, Jacobsen JT, Mano YM, et al. Visualizing antibody affinity maturation in germinal centers. Science. 2016;351(6277):1048–54.

57. Wardemann H, Yurasov S, Schaefer A, Young JW, Meffre E, Nussenzweig MC. Predominant autoantibody production by early human B cell precursors. Science. 2003;301(5638):1374–7.

58. Ersching J, Efeyan A, Mesin L, Jacobsen JT, Pasqual G, Grabiner BC, et al. Germinal Center Selection and Affinity Maturation Require Dynamic Regulation of mTORC1 Kinase. Immunity. 2017;46(6):1045-1058.